[5]H. A. Mavromatis and L. Zamick, Nucl. Phys. A104, 17 (1967).

[6]K. Shimizu, M. Ichimura, and A. Arima, Nucl. Phys. A226, 282 (1974).

[7]M. Chemtob and M. Rho, Nucl. Phys. A163, 1 (1971).

[8]A. Barroso and R. J. Blin-Stoyle, Nucl. Phys. A251, 446 (1975); R. J. Blin-Stoyle, Nucl. Phys. A254, 353 (1975).

[9]F. C. Khanna, I. S. Towner, and H. C. Lee, Nucl. Phys. A305, 349 (1978).

[10]J. S. Bell and R. J. Blin-Stoyle, Nucl. Phys. 6, 87 (1957); H. Ohtsubo, M. Sano, and M. Morita, Prog. Theor. Phys. 49, 877 (1973); N. C. Mukhopadhyay and L. D. Miller, Phys. Lett. 47B, 415 (1973).

[11]M. Rho, Nucl. Phys. A231, 493 (1974).

[12]For an earlier version, see I. S. Towner and F. C. Khanna, in Proceedings of the NATO Advanced Institute in Theoretical Physics, Banff, 1978, edited by B. Castel, F. Khanna, and B. Goulard (Plenum, New York, to be published).

[13]M. Rho, in Proceedings of the NATO Advanced Institute in Theoretical Physics, Banff, 1978, edited by B. Castel, F. Khanna, and B. Goulard (Plenum, New York, to be published); E. Oset and M. Rho, preceding Letter [Phys. Rev. Lett. 42, 47 (1979)].

[14]E. Grecksch, M. Dillig, and M. G. Huber, Phys. Lett. 72B, 11 (1977).

[15]G. E. Brown and W. Weise, Phys. Rep. 22C, 279 (1975); W. Weise, Nucl. Phys. A278, 402 (1977).

[16]In addition to the spin-spin central and tensor terms, vector mesons give rise to central spin-independent and spin-orbit terms, which have been retained in the present calculations even though their contributions are small. Note that the tensor part of the ρ-exchange potential is opposite in sign to that in π exchange, a property crucial for stabilizing the random-phase-approximation (RPA) calculations.

[17]A. Silverman, in *Proceedings of the Seventh International Symposium on Lepton and Photon Interactions at High Energies, Stanford, 1975,* edited by W. T. Kirk (SLAC, Stanford, Calif., 1975); M. Chemtob, in "Mesons in Nuclei," edited by D. H. Wilkinson and M. Rho (to be published).

[18]G. Höhler and E. Pietarinen, Nucl. Phys. B95, 210 (1975).

[19]P. J. Ellis and S. Siegel, Phys. Lett. 34B, 177 (1971).

[20]Equivalence of the nonrelativistic reduction of the pair term and the seagull term for axial-vector currents is proved by S. L. Adler [*Proceedings of the Sixth Hawaii Topical Conference in Particle Physics, Honolulu, 1975,* edited by P. N. Dobson, Jr., *et al.* (Univ. of Hawaii Press, Honolulu, Hawaii, 1976)]. See also M. Rho, in *Progress in Particle and Nuclear Physics,* edited by D. H. Wilkinson (Pergamon, New York, 1976), Vol. 1, for additional discussion of the seagull cancellation.

[21]Rho, Ref. 20.

[22]A. M. Green and T. H. Schucan, Nucl. Phys. A188, 289 (1972); M. Ichimura, H. Hyuga, and G. E. Brown, Nucl. Phys. A196, 17 (1972).

Nuclear Size Comparison of Even Titanium Isotopes Using 140-MeV α-Particle Scattering

P. L. Roberson, D. A. Goldberg, N. S. Wall, L. W. Woo, and H. L. Chen
Department of Physics and Astronomy, University of Maryland, College Park, Maryland 20742
(Received 24 October 1978)

Systematic variations in nuclear-matter distributions have been determined by analyzing the measured elastic scattering of 140-MeV alpha particles from ^{46,48,50}Ti. The "unique" optical potentials obtained ($J_R/4A \simeq 300$ MeV fm^3, $J_I/4A \simeq 100$ MeV fm^3) indicate that isotopic differences occur primarily in the strength of the imaginary potential. The rms matter radii increase with A, in contrast to those of the charge distributions. The matter-radius results are in agreement with Hartree-Fock calculations.

We have measured differential cross sections for elastic and inelastic scattering of 140-MeV α particles from the even isotopes of titanium in order to study the isotopic dependence of the scattering interaction (which relates nuclear properties to measured cross sections) and of relative nuclear structure properties. The sensitivity of such measurements to the radial shape of the effective scattering potentials has been demonstrated.[1-3] The detailed sensitivity of our data to the potential over a broad range of radii has been achieved by the use of α particles of sufficiently high energy to obtain "unique" optical-model potentials.[4] This sensitivity is used to determine isotopic shifts of nuclear-matter radii.

The experimental apparatus used in the present experiment has been described elsewhere.[5] The angular step size and resolution were 0.75° and 0.4° in the diffraction region (small angles) and 3° to 6° and 1.2° in the nuclear-rainbow region (large angles), respectively. The uncertainty in the scattering angle was ± 0.02°. The beam energy was determined to be 140.1 ± 0.5 MeV by two independent techniques. The targets were 5-mg/cm^2-thick self-supporting foils, isotopically enriched to 83.8%, 99.1%, and 83.2% for the

^{46}Ti, ^{48}Ti, and ^{50}Ti targets, respectively.

The uncertainties in the measured cross sections included contributions from statistics, angle accuracy, finite angular acceptance, target impurities, target isotopic impurities, and peak-fitting systematics. The minimum uncertainty was fixed at 1%, reflecting observed fluctuations in the monitor counter. The overall cross section normalizations for each target were allowed to vary within limits established by target nonuniformity measurements.

The measured elastic differential cross sections are shown in Fig. 1(a),[6] plotted as ratio to Rutherford cross section versus angle in the center-of-mass system. The isotopic dependence of the angular distributions is dominated by differences in cross-section magnitude. The approximately equal spacing at small to mid angles changes to unequal spacing at large angles.

Optical-model analyses were performed using standard six-parameter potentials:

$$V(r) = -V[f(r, r_R, a_R)]^n - iWf(r, r_I, a_I) + V_c(r),$$

where

$$f(r, r_0, a_0) = [1 + \exp\{(r - r_0 A^{1/3})/a_0\}]^{-1},$$

$V_c(r)$ is the electrostatic potential due to the nuclear charge distribution,[7] and n equals 1 or 2 for Woods-Saxon (WS) or Woods-Saxon–squared[1] (WS^2) parametrizations of the real form factor, respectively. Calculations used the computer code JIB3,[8] modified to incorporate additional optical-model parametrizations. A careful error analysis allowed the use of the χ^2 per degree of freedom (d.f.) as a true indication of quality of fit. In particular, the greater-than-unity χ^2/d.f. given in Table I are primarily due to the inability of either parametrization to fit adequately the amplitudes of the small oscillations (~ 35°) and the slope of the nuclear rainbow [see Fig. 1(b)].

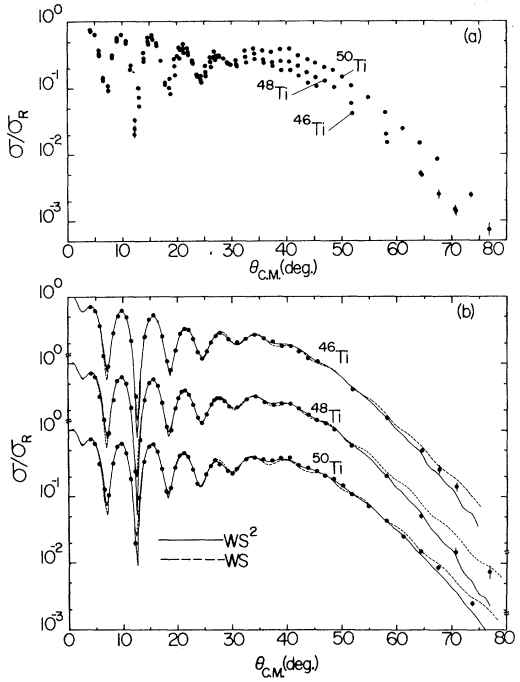

FIG. 1. (a) Measured ratio to Rutherford cross sections for the elastic α-particle scattering at 140 MeV from even isotopes of titanium. (b) Optical-model fits to the 140-MeV α-particle scattering data on even titanium isotopes. The fitted curves are generated with Woods-Saxon (WS) and Woods-Saxon–squared (WS^2) real form factors; Woods-Saxon imaginary form factors are used in both cases.

The best-fit potential parameters given in Table I show general trends common to both WS and WS^2 parametrizations. Gross features are as follows: (1) The rms radii (R_{rms}) for both real and imaginary form factors increase with A,

TABLE I. Potential parameters.

	V (MeV)	r_R (fm)	a_R (fm)	W (MeV)	r_I (fm)	a_I (fm)	$J^R/4A$ (MeV fm^3)	$R_{rms}{}^R$ (fm)	$J^I/4A$ (MeV fm^3)	$R_{rms}{}^I$ (fm)	χ^2/d.f.
						WS					
^{46}Ti	111.86	1.2619	0.7939	22.18	1.6295	0.6003	307.0	4.579	111.0	5.042	4.2
^{48}Ti	113.49	1.2650	0.7892	21.45	1.6344	0.5680	310.5	4.613	106.9	5.061	10.6
^{50}Ti	111.83	1.2835	0.7704	19.94	1.6437	0.5283	312.4	4.648	99.7	5.083	7.2
						WS^2					
^{46}Ti	136.17	1.4269	1.2201	24.79	1.5516	0.7022	295.9	4.452	112.3	5.034	2.9
^{48}Ti	138.07	1.4236	1.2144	22.64	1.5791	0.6526	297.8	4.481	105.3	5.063	2.5
^{50}Ti	136.04	1.4363	1.1825	20.91	1.5884	0.6253	301.2	4.513	97.6	5.092	2.2

though not as rapidly as $A^{1/3}$, in agreement with results of Fernandez and Blair;[9] this contrasts with the decrease in the rms radii of the charge distributions as measured by electron scattering.[7] (2) The volume integrals ($J/4A$) increase slightly with A for the real potential but decrease sharply for the imaginary potential. (3) The diffusitivities for both the α-nucleus potential and the charge distribution[7] decrease with A. These results indicate a contracting proton distribution and a decreasing diffuseness in the matter distribution as the neutron shell closes at ^{50}Ti. The optical-model parameters obtained by Rebel and co-workers[10] for data of 104-MeV α scattering from these isotopes do not display the simple trends noted above, but their results have large uncertainties.

The isotopic differences seen in the angular distributions shown in Fig. 1(a) are primarily due to changes in the strength of the imaginary potential (see Table I), while both real and imaginary form factors show similar shifts in geometry. In particular, *the similarity between the relative rms radii for both the real and imaginary form factors suggests that the (isotopic) differences in the rms radii are dominated by matter-distribution effects, with only minor contributions from the scattering interaction.* Also, the similar results obtained using either the WS or WS^2 parametrizations indicate that the model dependence of the isotopic shifts is small. We have therefore felt it justifiable to extract isotopic variations of the rms radii of the matter distributions (see Table II) from those obtained for the potentials.

The chosen relationship between the rms radii of the form factors and the rms radii of the matter distributions was motivated by the folding-model[11] description of the real form factor: The matter mean-square (ms) radius equals the (real or imaginary) form-factor ms radius minus the ms radius of an (isotopically constant, real or imaginary) effective interaction. The resulting isotopic shifts are approximately independent of the magnitude of the radii of the effective interactions. The derived isotopic shifts of the matter rms radii (column 4, Table II) are a weighted average of the results using both real and imaginary form factors for the WS^2 parametrization. The relative weighting was fixed at the approximate ratio of the volume integrals, but the results are insensitive to the choice of weighting: The difference between the values derived from the real form factor alone and those from both form factors with equal weighting is at most 3×10^{-3} fm. The quoted errors only reflect uncertainties occurring within the constraints imposed by the form-factor parametrizations and ignore any isotropic dependence of the relation between the form of the potential and the matter distributions.

Hartree-Fock calculations using the density-matrix expansion technique[12] are presented for the isotopic shifts of the rms radii of both the point matter (column 5, Table II) and the charge (column 7) distributions. The calculations are within even the minimum error bars for the deduced matter isotopic shifts, but do not reproduce the decrease in the charge radii[13] (column 6) observed in electron-scattering experiments.[7]

Differential cross sections for the excitation of the first excited (2^+) states are shown in Fig. 2.[6] At small angles, cross-section magnitudes increase with decreasing state excitation ener-

TABLE II. rms-radii isotopic shifts. ΔR_{rms} defines the change in the rms radius from isotope A to isotope B. R and I are the real and imaginary form factors using WS^2 parametrization, M is the point matter distributions, and C is the charge distribution. All values are in 10^{-3} fm.

			$\Delta R_{\mathrm{rms}}{}^{M}$		$\Delta R_{\mathrm{rms}}{}^{C}$	
$A-B$	$\Delta R_{\mathrm{rms}}{}^{\mathrm{R}}$	$\Delta R_{\mathrm{rms}}{}^{\mathrm{I}}$	Expt.[a]	Theor.[b]	Expt.[c]	Theor.[b]
48–46	29	29	37[d]	33	-13 ± 6	2
50–48	32	29	40[d]	32	-19 ± 6	3
50–46	61	58	78[d]	65	-26 ± 8	5

[a] $R_{\mathrm{rms}}{}^{M}\equiv\frac{3}{4}[(R_{\mathrm{rms}}{}^{\mathrm{R}})^2-(R_{\mathrm{rms}}{}^{\alpha\mathrm{R}})^2]^{1/2}+\frac{1}{4}[(R_{\mathrm{rms}}{}^{\mathrm{I}})^2-(R_{\mathrm{rms}}{}^{\alpha\mathrm{I}})^2]^{1/2}$, where the $R_{\mathrm{rms}}{}^{\alpha\mathrm{R,I}}$ are fixed to reproduce the Hartree-Fock point-matter values for ^{46}Ti ($R_{\mathrm{rms}}{}^{\mathrm{HF}}=3.552$, $R_{\mathrm{rms}}{}^{\alpha\mathrm{R}}=2.684$, and $R_{\mathrm{rms}}{}^{\alpha\mathrm{I}}=3.567$ fm).

[b] Ref. 12.

[c] Weighted average of elastic electron-scattering results (Ref. 7).

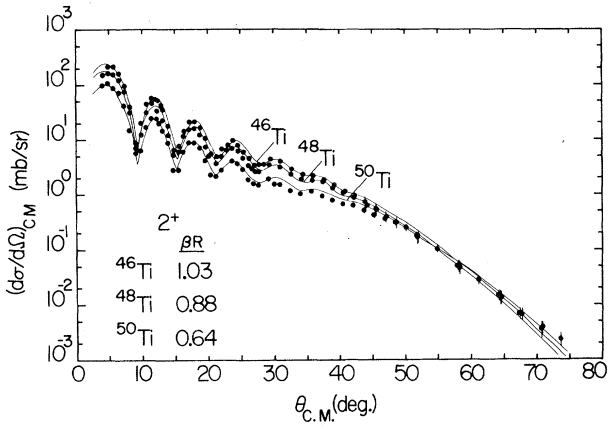

FIG. 2. Measured cross sections for inelastic scattering to the first excited (2^+) states of the even isotopes of titanium. Curves shown are DWBA calculations using the elastic-scattering optical potentials. βR is the deformation length obtained by normalizing the DWBA curve to the data (see text).

gies. A distorted-wave Born-approximation (DWBA) analysis was performed using the standard derivative form for the nuclear excitation potential[5] with the strength proportional to a deformation length (R), which was assumed constant for the real and imaginary potential distributions[14]: $\beta R = \beta_R R_R = \beta_I R_I$, where $R_0 = r_0 A^{1/3}$ for each distribution. The deformation lengths were determined by normalizing the DWBA curves to the small-angle maxima and are presented in Fig. 2, inset. Coupled-channels calculations including only the 2^+ and elastic channels confirm that most of the isotopic variation present in the strength of the imaginary potential is due to the coupling of the 2^+ and elastic channels. Modifications to the elastic-channel imaginary form factor required by the coupling of the 2^+ channel change the isotopic shift of the rms radius by an amount comparable to the errors assigned to the imaginary part.

Work is presently underway to improve the reliability of the derived isotopic shifts of the matter rms radii. Model-independent analyses of the form factors will provide improved sensitivity estimates to the moments of the radial distributions. Folding-model calculations will make the relationship between the real form factor and the matter distribution more quantitative, although uncertainties will likely remain as a result of the reduced quality of fit to the data typical of such calculations. Finally, redoing the experiment for other incident energies will provide consistency checks on our analysis.

We gratefully acknowledge the support of the University of Maryland Computer Science Center for part of the computer calculations. This work was supported in part by the National Science Foundation.

[1]D. A. Goldberg, Phys. Lett. 55B, 59 (1975).
[2]L. W. Put and A. M. J. Paans, Nucl. Phys. A291, 93 (1977).
[3]A. A. Cowley and N. S. Wall, Phys. Rev. C 17, 1322 (1978).
[4]D. A. Goldberg and S. M. Smith, Phys. Rev. Lett. 29, 500 (1972).
[5]D. A. Goldberg, S. M. Smith, H. G. Pugh, P. G. Roos, and N. S. Wall, Phys. Rev. C 7, 1938 (1973).
[6]To obtain tabulated cross sections, write to one of the authors or to the Department of Physics and Astronomy, University of Maryland, College Park, Md. 20742, and request University of Maryland Technical Report No. 79-038 (unpublished).
[7]E. F. Romberg, N. S. Wall, D. Blum, J. W. Lightbody, Jr., and S. Penner, Nucl. Phys. A173, 124 (1971); J. Heisenberg, R. Hofstadter, J. S. McCarthy, R. Herman, B. C. Clark, and D. G. Ravenhall, Phys. Rev. C 6, 381 (1972).
[8]F. G. Perey, private communication (unpublished).
[9]B. Fernandez and J. S. Blair, Phys. Rev. C 1, 523 (1970).
[10]H. Rebel, G. Hauser, G. W. Schweimer, G. Nowicki, W. Weisner, and D. Hartmann, Nucl. Phys. A218, 13 (1974).
[11]D. F. Jackson and V. K. Kembhavi, Phys. Rev. 178, 1626 (1969).
[12]J. W. Negele and D. Vautherin, Phys. Rev. C 5, 1472 (1972); computer work by L. Ray, private communication.
[13]The discrepancy for relative charge radii is not surprising because the Hartree-Fock calculations of Ref. 12 were adjusted to reproduce the charge rms radii of selected *spherical* nuclei.
[14]J. S. Blair, in *Direct Interactions and Nuclear Reaction Mechanism*, edited by E. Clementel and C. Villi (Gordon and Breach, New York, 1963), p. 669; A. M. Bernstein, Adv. Nucl. Phys. 3, 325 (1969); D. L. Hendrie, Phys. Rev. Lett. 31, 478 (1973).